



Available online at <http://scik.org>

Commun. Math. Biol. Neurosci. 2023, 2023:3

<https://doi.org/10.28919/cmbn/7820>

ISSN: 2052-2541

AN OPTIMAL CONTROL OF PREVENTION AND TREATMENT OF COVID-19 SPREAD IN INDONESIA

JONNER NAINGGOLAN^{1,*}, JOKO HARIANTO¹, HENGKI TASMAN²

¹Department of Mathematics, Faculty of Mathematics and Natural Sciences, University Cenderawasih, Jayapura,
99332, Papua, Indonesia

²Department of Mathematics, Faculty of Mathematics and Natural Sciences, University Indonesia, Depok, 16424,
Indonesia

Copyright © 2023 the author(s). This is an open access article distributed under the Creative Commons Attribution License, which permits unrestricted use, distribution, and reproduction in any medium, provided the original work is properly cited.

Abstract: In this paper we analyze COVID-19 spread in Indonesia using an epidemiological model. We consider symptomatic and asymptomatic infections in the model. We analyze the equilibria of the model and their stability which depend on the basic reproduction ratio for symptomatic and asymptomatic infections. Furthermore, we use optimal control in prevention and treatment in decreasing the number of positive COVID-19 patients in Indonesia. Furthermore, we analyze the existence of optimal control using the Pontryagin minimum principle. We also give numerical simulation of COVID-19 spread with and without the control. According to the simulation, COVID-19 spread could be reduced by using prevention and treatment control simultaneously.

Keywords: COVID-19; basic reproduction ratio; equilibria; local stability; optimal control; prevention; treatment.

2020 AMS Subject Classification: 92D25, 93A30.

*Corresponding author

E-mail address: jonner2766@gmail.com

Received November 11, 2022

1. INTRODUCTION

Coronavirus Disease (COVID-19) is caused by the severe acute respiratory syndrome corona virus. It can cause respiratory system disorder, ranging from mild symptoms such as flu, to lung infection. The control of COVID-19 spread has been carried out by government and private agencies. The government conducts domestic, regional and inter-country lock downs. Due to COVID-19, many people died and caused economic losses globally.

Mathematical experts have studied models of COVID-19 spread, such as: model of the spread of COVID-19 by considering to asymptomatic, symptomatic infections and waning immunity [1], SIR and SEIR types of COVID-19 models in unreported infected populations with outbreak factors [2], model of the spread of COVID-19 in Ghana by considering government intervention on the community [3], model of the COVID-19 pandemic in Nigeria with regard to social distancing, lock down and non-pharmaceutical interventions [4].

Following models also discuss COVID-19 spread, its treatment and interventions. Model of COVID-19 in the United Kingdom in 2021-2022 with intervention, social distancing, relaxation and no treatment [5]. Stochastic model of COVID-19 spread in Sri Lanka [6]. Model of the dynamics of the spread of COVID-19 by taking into account the isolation subpopulation [7]. Model for predicting the increase and decrease in the second wave of COVID-19 spread in Malaysia [8]. Basnarkov (2021) examines the model of the spread of COVID-19 in the SEAIR type at continuous and discrete times [9]. Nainggolan (2022) analyzes the model of COVID-19 type $SI_hI_cQ_hQ_HR$ with attention congenital disease [10].

Study of the model for the spread of COVID-19 with the assumption of a public knowledge and awareness campaign in Negeria in 2020 [11]. Determining parameter estimates and numerical simulations from a model of the spread of COVID-19 in China by taking into account undetected disease cases [12]. Bifurcation, parameter estimation and prediction of the spread of COVID-19 disease with regard to treatment that cannot predict cure presentation [13].

Stability analysis and numerical simulation, determining the basic reproduction number

with the Lyapunov function on the COVID-19 spread model in Indonesia [14]. Mathematical model to determine the basic reproduction number in the dynamics of COVID-19 transmission in Pakistan by paying attention to social distancing [15]. Chen Tian-Mu simulated the basic reproduction number from the phase-based transmission model of COVID-19 [16]. Kim studied the two-patch mathematical model to determine the basic reproduction number on the dynamics of transmission of COVID-19 in South Korea by paying attention to early diagnostic interventions, mobility, cumulative incidence, social distancing [17]. Comparing the basic reproduction ratio of COVID-19 with SARS in Wuhan China and international [18].

Strategies to reduce the spread of disease control efforts can be made. Mathematical model for the spread of the dynamics of COVID-19 in Indonesia with government intervention to control the prevention of social distancing, lock down and treatment [19]. Research on the COVID-19 model type SEQIAHR COVID-19, to find out the dynamics of the disease and strategies to cope with minimizing the pandemic [20]. Optimal control study, sensitivity analysis and detecting the spread of COVID-19 in Indian states [21]. Study of optimal control, model-fitting Basic reproduction number Global stability in preventing the spread of COVID-19 in Nigeria [22]. Optimal control and sensitivity analysis on the dynamics of COVID-19 by considering the decrease in body immunity in West Java, Indonesia [23].

The model studied in this paper, takes into account the quarantined subpopulation and vaccination of the susceptible subpopulation. Next, we examine the optimal control of the prevention and treatment of COVID-19 using data in Indonesia.

Based on the study of the spread of COVID-19 type SEAIR [9], the authors developed the SEAILR model by considering the self-quarantine subpopulation (L), transfer from subpopulation subpopulation A , due to the fact that in Indonesia many COVID-19 patients are not reported to the base. COVID-19 datago.id. This self-quarantine subpopulation (L) is important to note, because real data in Indonesia, individuals infected with COVID-19 without comorbidities, are generally isolated independently in their respective homes because

individuals infected with COVID-19 without comorbid diseases can recover with consume nutritious food and drinks, take multi vitamins, maintain health protocols, get enough rest, and keep exercising. So the novelty of the dynamic model on the spread of COVID-19 that is studied in this article by paying attention to the individual self-isolation subpopulation (L), and has not been studied in previous articles.

2. MODEL FORMULATION AND ANALYSIS

We assume that human population is homogenous. We divide the population into six subpopulations, which are the susceptible subpopulation S , the exposed subpopulation E , the symptomatic COVID-19 infectious subpopulation A , the asymptomatic COVID-19 infectious subpopulation I , the quarantined COVID-19 subpopulation L and the COVID-19 recovered subpopulation R .

We also assume that recovered hosts have permanent immunity. Meanwhile, the quarantine for COVID-19 takes place in hospitals. The quarantined hosts get proper treatment in hospitals. We use transmission diagram as Figure 1 for model construction. Description of parameters could be seen in Table 1. All of the parameters are constant and positive.

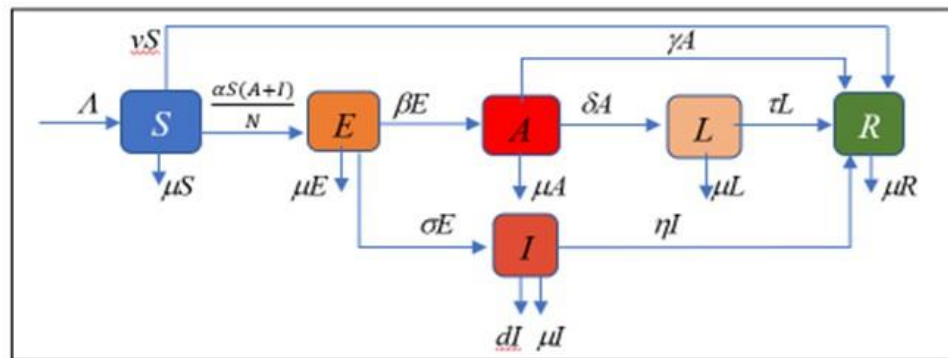


Figure 1. Transmisi diagram of COVID-19 spread

Table 1. Description of parameters

Parameter	Description	Value	Reference
Λ	Recruitment rate	422	[5]
α	Infection rate	0.95	[26]
ν	Vaccination rate	0,7	[1]
μ	Natural death rate	0.00712	[26]
β	Symptomatic transition rate	0.192	[5]
σ	Asymptomatic transition rate	0.4	[26]
δ	Quarantine rate	0.1	[5]
d	COVID-19-death rate	0.002	[1]
η	Asymptomatic self-recovery rate	0.086	[26]
τ	Quarantined recovery rate	0.1	[5]
γ	Symptomatic self-recovery rate	0.075	[26]

Based on the assumptions and transmission diagram, we construct a 6-d non-linear dynamical system using ordinary differential equations for capturing the COVID-19 spread in population as following.

$$\begin{aligned}
\frac{dS}{dt} &= \Lambda - \frac{\alpha S(A+I)}{N} - (\nu + \mu)S \\
\frac{dE}{dt} &= \frac{\alpha S(A+I)}{N} - (\beta + \sigma + \mu)E \\
\frac{dA}{dt} &= \beta E - (\gamma + \delta + \mu)A \\
\frac{dI}{dt} &= \sigma E - (d + \mu + \eta)I \\
\frac{dL}{dt} &= \delta A - (\tau + \mu)L \\
\frac{dR}{dt} &= \nu S + \gamma A + \tau L + \eta I - \mu R
\end{aligned} \tag{1}$$

where $N = S + E + A + I + L + R$ is the total population. System (1) has the disease-free equilibrium

$$P_0 = \left(\frac{\Lambda}{v+\mu}, 0, 0, 0, 0, \frac{\Lambda v}{\mu(v+\mu)} \right) \quad (2)$$

Basic reproduction ratio is an important threshold in mathematical epidemiology. It denotes the expectation number of secondary cases caused by primary cases during its infectious period in a susceptible population [24]. The basic reproduction ratio for COVID-19 spread based on model (1) is

$$R_0 = R_{0a} + R_{0s},$$

where

$$R_{0a} = \frac{\mu\alpha\beta}{(v+\mu)(\beta+\sigma+\mu)(\gamma+\delta+\mu)}$$

$$R_{0s} = \frac{\mu\alpha\sigma}{(v+\mu)(\beta+\sigma+\mu)(d+\delta+\eta)}.$$

The ratio R_{0a} is interpreted as the basic reproduction ratio for asymptomatic COVID-19 infection and the ratio R_{0s} as the basic reproduction ratio for symptomatic COVID-19 infection. The local stability of the equilibrium P_0 depends on the basic reproduction ratio. The local stability is stated in following theorem.

Theorem 1. *The disease-free equilibrium P_0 is locally asymptotically stable if $R_0 < 1$.*

Proof. To analyze the local stability of the equilibrium P_0 , we linearize system near the equilibrium P_0 . From the linearization, we get following characteristic equation

$$(\lambda + \mu)(\lambda + \mu + v)(\lambda + \mu + \tau)(\lambda^3 + a_2\lambda^2 + a_1\lambda + a_0) = 0, \quad (3)$$

where

$$a_2 = \beta + d + \delta + \eta + \gamma + 3\mu + \sigma,$$

$$a_1 = (\beta + \sigma + \mu)(\gamma + \delta + \mu)(1 - R_{0s}) + (d + \mu + \eta)(1 - R_{0a}) + (\gamma + \delta + \mu)(d + \mu + \eta),$$

$$a_0 = -(d + \eta + \mu)(\delta + \gamma + v)(\beta + \mu + \sigma)(R_{0a} - 1).$$

It is clear that the first three terms of equation (3) give three negative roots.

Using the Routh-Hurwitz Criteria, the real part of the roots of the cubic polynomial are negative if $R_0 < 1$. Descartes' rule of sign also confirms that there is no positive root of the cubic polynomial because all of the cubic polynomial's coefficients and constant are positive for $R_0 < 1$.

Hence, the disease-free equilibrium P_0 is locally asymptotically stable if $R_0 < 1$. \square

Furthermore, system (1) has the endemic equilibrium $P_1 = (S^*, E^*, A^*, I^*, L^*, R^*)$, where,

$$\begin{aligned} S^* &= \frac{\Lambda[(\beta+\mu)(d+\eta+\mu)+\sigma(\eta+\mu)]}{(v+\mu)(d+\mu+v)[\beta+\mu+(\beta+\delta+\mu)(R_0-1)+\sigma(v+\mu)(\eta+\mu)}, \\ E^* &= \frac{\Lambda(d+\eta+\mu)(R_0-1)}{(d+\mu+\eta)[\beta+\mu+(\beta+\sigma+\mu)(R_0-1)]+\sigma(\eta+\mu)}, \\ A^* &= \frac{\beta\Lambda(d+\eta+\mu)(R_0-1)}{(\gamma+\delta+\mu)(d+\mu+\eta)[\beta+\mu+(\beta+\sigma+\mu)(R_0-1)]+\sigma(\gamma+\delta+\mu)(\eta+\mu)}, \\ I^* &= \frac{\Lambda\sigma(R_0-1)}{(d+\mu+\eta)[\beta+\mu+(\beta+\sigma+\mu)(R_0-1)]+\sigma(\eta+\mu)}, \\ L^* &= \frac{\beta\delta\Lambda(d+\eta+\mu)(R_0-1)}{(\gamma+\delta+\mu)(\eta+\mu)[(d+\mu+\eta)(\beta+\mu+(\beta+\sigma+\mu)(R_0-1)]+\sigma(\eta+\mu)}, \\ R^* &= \frac{vS^*+\gamma A^*+\tau L^*+\eta I^*}{\mu}. \end{aligned}$$

It is clear that the endemic equilibrium P_1 exists and has biological meaning if $R_0 > 1$. The local stability of equilibrium P_1 is as following.

Theorem 2. *The endemic equilibrium P_1 is locally asymptotically stable if $R_0 > 1$ and $\psi < 1$,*

and $b_2 b_1 > b_0$ where $\psi = \frac{d\delta}{(d+\mu+\eta)(\beta+\sigma+\mu)}$, $\varepsilon = \frac{v+\mu}{\mu} > 1$, $p = d + \delta + \eta > 0$, $q = \beta + \sigma + \mu >$

0, $m = v + \mu >$, $h = (\beta + \mu)(\gamma + \delta + \mu)(d + \mu + \eta) > 0$, $k = \beta(d + \mu + \eta) +$

$\sigma(\gamma + \delta + \mu) > 0$, $R_{0\sigma} = \frac{\mu\alpha\sigma}{(v+\mu)(\beta+\mu)(d+\delta+\eta)} < R_0$,

$$b_0 = \frac{hm\varepsilon pq(1-\psi)(R_0-R_{0\sigma})+\alpha km pq(R_0-1)}{h\varepsilon R_0(1-\psi)} > 0.$$

$$b_1 = \frac{h(1-\psi)(R_0\varepsilon mp+R_0\varepsilon mq+\varepsilon pq(R_0-R_{0\sigma}))+\alpha km(p+q)(R_0-1)}{h\varepsilon R_0(1-\psi)} > 0,$$

$$b_2 = \frac{h\varepsilon R_0(1-\psi)(p+q+m)+\alpha km(R_0-1)}{h\varepsilon R_0(1-\psi)} > 0.$$

Proof. Variable R only appears at the last equation of system (1), so we could decouple variable R for the stability analysis of equilibrium P_1 . We obtain characteristic polynomial as follow.

$$H(\lambda) = (\lambda + \gamma + \delta + \mu)(\lambda + \tau + \mu)(\lambda^3 + b_2\lambda^2 + b_1\lambda + b_0) \quad (4)$$

where $\psi = \frac{d\delta}{(d+\mu+\eta)(\beta+\mu)}$, $\varepsilon = \frac{v+\mu}{\mu} > 1$, $p = d + \delta + \eta > 0$, $q = \beta + \sigma + \mu > 0$, $m = v +$

$\mu > 0$, $h = (\beta + \mu)(\gamma + \delta + \mu)(d + \mu + \eta) > 0$, $k = \beta(d + \mu + \eta) + \sigma(\gamma + \delta + \mu) > 0$,

$$R_{0\sigma} = \frac{\mu\alpha\sigma}{(v+\mu)(\beta+\mu)(d+\delta+\eta)} < R_0.$$

If $R_0 > 1$ and $\psi < 1$, then $b_0 > 0$, $b_1 > 0$, and $b_2 > 0$. Moreover, if $b_2 b_1 > b_0$, then according to Routh-Hurwitz Criteria, the eigen values of the cubic polynomial are negative. Hence, the equilibrium P_1 is locally asymptotically stable if $R_0 > 1$. \square

Our numerical simulation supports the local stability of equilibria of model (1) which obtained analytically. We use parameters' value as in Table 1 for low transmission of COVID-19.

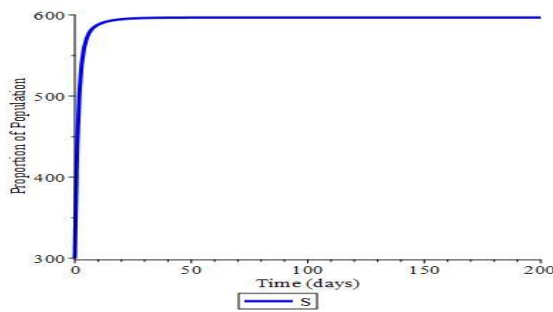


Figure 2. Dynamical population of S where $R_0 = 0,05$

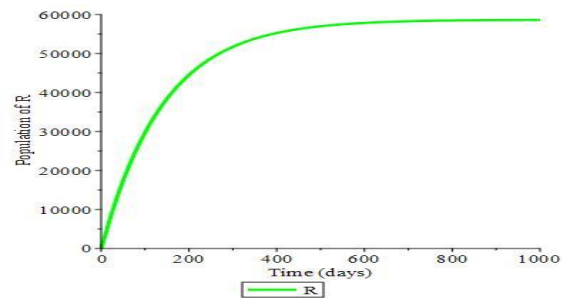


Figure 3. Dynamical population of R where $R_0 = 0,05$

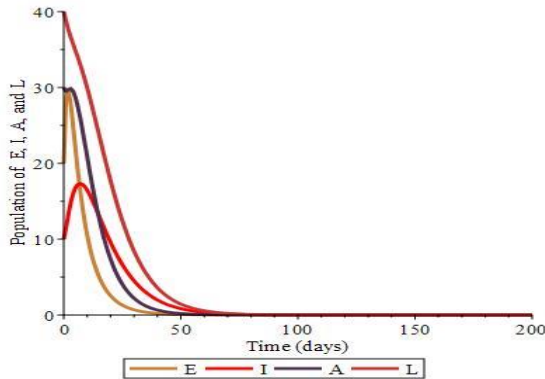


Figure 4. Dynamical population of E , A , I , and L where $R_0 = 0,05$

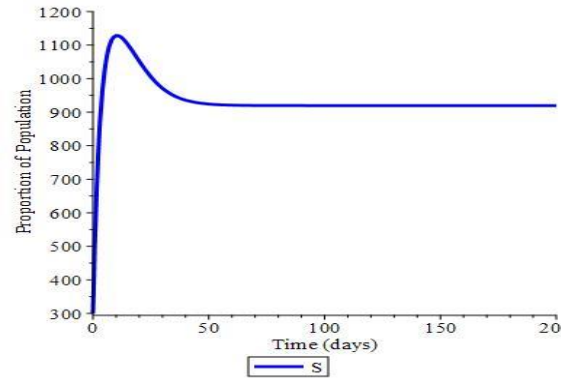


Figure 5. Dynamical population of S where $R_0 = 2,5$

It generates $R_0 = 0.05 < 1$ and the disease-free equilibrium $P_0 = (596, 0, 0, 0, 0, 58672)$ which is locally asymptotically stable (see Figure 2, Figure 3 and Figure 4).

PREVENTION AND TREATMENT OF COVID-19 SPREAD IN INDONESIA

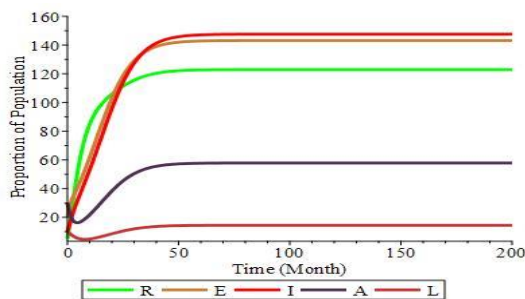


Figure 6. Dynamical population of E , A , I , L , and R where $R_0 = 2,5$

It generates $R_0 = 0.05 < 1$ and the disease-free equilibrium $P_0 = (596, 0, 0, 0, 0, 58672)$ which is locally asymptotically stable (see Figure 2, Figure 3 and Figure 4).

Parameters' value for high transmission of COVID-19 are as follow. $\Lambda = 422$, $\beta = 0.192$, $\delta = 0.1$, $\tau = 0.1$ [5]. $\nu = 0.02$, $\mu = 0.03$ (assumption), and $\alpha = 0.95$, $\sigma = 0.4$, $\gamma = 0.075$, $\eta = 0.086$ [26]. Using this set of values, we obtain $R_0 = 2.5$, the disease-free equilibrium $P_0(1318, 0, 0, 0, 0, 87)$ which is unstable and the endemic equilibrium $P_1(919, 143, 57, 147, 14, 122)$ which is locally asymptotically stable (see Figure 5 and Figure 6).

3. AN OPTIMAL CONTROL OF COVID-19 SPREAD IN INDONESIA

To optimize the prevention and vaccination of COVID-19 spread, the following controls are given.

1. Control u_1 is a vaccination control for susceptible subpopulation S .
2. Control u_2 is a counseling control to always wear a mask when leaving the house, always wash hands after handling an object, keep a minimum distance of 2 meters and avoid crowds of people, in an effort to prevent contact between individuals who have experienced symptoms and who are confirmed positive with individuals who are still healthy but are already suspected COVID-19.
3. Control u_3 is a treatment control by giving extra food and vitamin to speed up healing process of quarantined COVID-19 subpopulation L .
4. Control u_4 is a treatment control by giving extra food and vitamin to speed up healing

process of asymptomatic COVID-19 subpopulation I .

Using the controls, model (1) becomes as following.

$$\begin{aligned}
\frac{dS}{dt} &= \Lambda - \frac{\alpha(1-u_1)S(A+I)}{N} - (v(1+u_2) + \mu)S \\
\frac{dE}{dt} &= \frac{\alpha(1-u_1)S(A+I)}{N} - (\beta + \sigma + \mu)E \\
\frac{dA}{dt} &= \beta E - (\gamma + \delta + \mu)A \\
\frac{dI}{dt} &= \sigma E - (d + \mu + \eta(1+u_4))I \\
\frac{dL}{dt} &= \delta A - (\tau(1+u_3) + \mu)L \\
\frac{dR}{dt} &= v(1+u_2)S + \gamma A + \tau(1+u_3)L + \eta(1+u_4)I - \mu R
\end{aligned} \tag{5}$$

The goals of optimal control are to reduce contact between infected and healthy individuals, optimize the immunity of vaccinated individuals, and increase the number of individuals infected with COVID-19.

The solution of system (5) uses the Pontryagin Maximum Principle method. Solving the system with a flow from right to left, while the completion of the adjoint function from left to right with the transversality condition [33, 34]. The objective function is to minimize

$$\begin{aligned}
J(u_1, u_2, u_3, u_4) &= \int_0^{t_f} (A_1 E(t) + A_2 A(t) + A_3 I(t) + C_1 u_1^2(t) + C_2 u_2^2(t) + C_3 u_3^2(t) \\
&\quad + C_4 u_4^2(t)) dt
\end{aligned} \tag{6}$$

subject to system (5), where t_f is the ending time, A_1, A_2, A_3 are the administrative cost weights for each subpopulation E, A dan I respectively. Moreover, C_1, C_2, C_3, C_4 are cost weights u_1, u_2, u_3, u_4 respectively. The objective of the control model is to identify an optimal control

$$J(u_1^*, u_2^*, u_3^*, u_4^*) = \min \{(u_1, u_2, u_3, u_4) : u_1, u_2, u_3, u_4 \in \Phi\} \tag{7}$$

where controls $\Phi = \{u_i : 0 \leq u_i \leq 1, \text{ Lebesgue measurable } t = [0, t_f], \text{ untuk } i = 1, 2, 3, 4\}$, subject to the system (5) with initial conditions. Next, we analyze the existence of optimal

control that u_1, u_2, u_3, u_4 minimizes (6) subject to model (5).

Theorem 3. *The optimal prevention and treatment control $U = (u_1(t), u_2(t), u_3(t), u_4(t))$ exists and can minimize the performance index (6) subject to model (5), given that the properties are following.*

1. *The set of control U is convex,*
2. *The right hand side of system (5) is linear with coefficients depending on the state and time variables,*
3. *Function on the right side of the performance index (6) is convex with respect to the controls,*
4. *There exists constants $k_1, k_2 \geq 0$ and $k_3 \geq 1$, so that the integrand of performance index (6) is bounded below by quantity $k_1(\sum_{i=1}^4 |u_i|^2)^{k_3/2} - k_2$.*

Proof.

(a) Take anything $u_a = (u_{11}, u_{12}, u_{13}, u_{14})$, $u_b = (u_{21}, u_{22}, u_{23}, u_{24})$ with $[a_i, b_i] \subset [a, b]$, $i = 1, 2, 3, 4$, will be shown $z = \varepsilon u_a + (1 - \varepsilon)u_b \in U$, with $0 \leq \varepsilon \leq 1$. $z = \varepsilon u_a + (1 - \varepsilon)u_b = (\varepsilon u_{11} + (1 - \varepsilon)u_{21}, \varepsilon u_{12} + (1 - \varepsilon)u_{22}, \varepsilon u_{13} + (1 - \varepsilon)u_{23}, \varepsilon u_{14} + (1 - \varepsilon)u_{24})$. Because $a_i \leq \varepsilon u_{1i} + (1 - \varepsilon)u_{2i} \leq b_i$, then $u_{1i} + (1 - \varepsilon)u_{2i} \in [a_i, b_i] \subset [a, b]$ so that $z = \varepsilon u_a + (1 - \varepsilon)u_b \in [a, b] \subset U$.

(b) The system of equations (5) can be written in the matrix equation $\dot{x}(t) = Bx(t)$, with

$$B = \begin{bmatrix} \theta - a_1 - a_2 & 0 & 0 & 0 & 0 & 0 \\ a_1 + a_2 & -b_1 & 0 & 0 & 0 & 0 \\ 0 & \beta & -c_1 & 0 & 0 & 0 \\ 0 & \sigma & 0 & -d_1 & 0 & 0 \\ 0 & 0 & 0 & \delta & -e_1 & 0 \\ f_1 & 0 & \gamma & f_3 & f_2 & -\mu \end{bmatrix}$$

with $A = \theta S$, $a_1 = \alpha(1 - u_1)\frac{\Lambda}{N}$, $a_2 = \alpha(1 - u_1)\frac{I}{N}$, $a_3 = v(1 + u_2) + \mu$,

$b_1 = \beta + \sigma + \mu$, $c_1 = \gamma + \delta + \mu$, $d_1 = d + \mu + \eta(1 + u_4)$, $e_1 = \tau(1 + u_3) + \mu$,

$f_1 = v(1 + u_2)$, $f_2 = \tau(1 + u_2)$, and $f_3 = \eta(1 + u_4)$,

$x(t) = [S(t) \ E(t) \ A(t) \ I(t) \ L(t) \ R(t)]^T$, $\dot{x}(t) = \left[\frac{dS}{dt} \ \frac{dE}{dt} \ \frac{dA}{dt} \ \frac{dI}{dt} \ \frac{dL}{dt} \ \frac{dR}{dt} \right]^T$.

So the right-hand side function of the system of equations (5) is linear with the coefficients depending on the state and time variables.

- (c) Take any $(u_{i1}, u_i, u_{i3}, u_{i4}) \in [a_i, b_i]$, $i = 1, 2$, $0 \leq \varepsilon \leq 1$ and $J(u_1, u_2, u_3, u_4) = \int_0^{t_f} (A_1 E(t) + A_2 A(t) + A_2 I(t) + C_1 u_1^2(t) + C_2 u_2^2(t) + C_3 u_3^2(t) + C_4 u_4^2(t)) dt$, will be shown $J(\varepsilon u_{11}(t) + (1 - \varepsilon)u_{21}(t), \varepsilon u_{12}(t) + (1 - \varepsilon)u_{22}(t), \varepsilon u_{13}(t) + (1 - \varepsilon)u_{23}(t), \varepsilon u_{14}(t) + (1 - \varepsilon)u_{24}(t)) \leq \varepsilon J(u_{11}(t), u_{12}(t), u_{13}(t), u_{14}(t)) + (1 - \varepsilon)J(u_{21}(t), u_{22}(t), u_{23}(t), u_{24}(t))$. $\int_0^{t_f} (A_1 E(t) + A_2 A(t) + A_2 I(t) + C_1(\varepsilon u_{11}(t) + (1 - \varepsilon)u_{21}(t))^2 + C_2(\varepsilon u_{12}(t) + (1 - \varepsilon)u_{22}(t))^2 + C_3(\varepsilon u_{13}(t) + (1 - \varepsilon)u_{23}(t))^2 + C_4(\varepsilon u_{14}(t) + (1 - \varepsilon)u_{24}(t))^2) dt \leq \varepsilon \int_0^{t_f} ((A_1 E_2(t) + A_2 I_2(t) + C_1(u_{11}(t))^2 + C_2(u_{12}(t))^2 + C_3(u_{13}(t))^2 + C_4(u_{14}(t))^2) dt + (1 - \varepsilon) \int_0^{t_f} (A_1 E_2(t) + A_2 I_2(t) + (C_1(u_{21})^2 + C_2(u_{22})^2 + C_3(u_{23})^2 + C_4(u_{24})^2) dt$. Because $0 \leq \varepsilon \leq 1$, and $0 \leq u_i \leq 1$, $i = 1, 2, 3, 4$ [20] and $A_1, A_2, A_3, C_1, C_2, C_3, C_4 \geq 1$, then $J(\varepsilon u_{11}(t) + (1 - \varepsilon)u_{21}(t), \varepsilon u_{12}(t) + (1 - \varepsilon)u_{22}(t), \varepsilon u_{13}(t) + (1 - \varepsilon)u_{23}(t), \varepsilon u_{14}(t) + (1 - \varepsilon)u_{24}(t)) \leq \varepsilon J(u_{11}(t), u_{12}(t), u_{13}(t), u_{14}(t)) + (1 - \varepsilon)J(u_{21}(t), u_{22}(t), u_{23}(t), u_{24}(t))$.

- (d) Define the Lagrange function as $L(t, y, u) = r_1(t, y) + r_2(t, y)$, with $r_1(t, y) = A_1 E + A_2 A + A_3 I$, with A_1, A_2 and A_3 are the administrative cost weight of each E, A and I subpopulation, $r_2(t, y) = \sum_{i=1}^4 C_i u_i$, with C_i respectively are the control cost weights u_i . Clear that $L(t, y, u) \geq r_1(t, y)$, so that it can be written

$$L(t, y, u) \geq \sum_{i=1}^4 C_i u_i^2 \geq k_1 (\sum_{i=1}^4 |u_i|^2)^{k_3/2} - k_2,$$

with $k_1 = \min \{C_1, C_2, C_3, C_4\}$, $k_2 > 0$ and $k_3 = 4$. The proof is complete. \square

3.1. Characterization of Optimal Controls.

To reduce the number of individuals infected with COVID-19 we use the Pontryagin Maximum Principle [22, 23, 25]. The principle use Hamiltonian function with respect to the controls (u_1, u_2, u_3, u_4) . The Hamiltonian function is as follow.

$$\begin{aligned}
H = & [A_1E + A_2A + A_2I + C_1u_1^2 + C_2u_2^2 + C_2u_3^2 + C_4u_4^2] + \lambda_1 \frac{dS}{dt} + \lambda_2 \frac{dE}{dt} + \lambda_3 \frac{dA}{dt} \\
& + \lambda_4 \frac{dI}{dt} + \lambda_5 \frac{dL}{dt} + \lambda_6 \frac{dR}{dt},
\end{aligned} \tag{8}$$

where $\lambda_1, \lambda_2, \lambda_3, \lambda_4, \lambda_5, \lambda_6$ are the co-state variables.

Substituting model (5) into equation (8), we obtain following Hamiltonian function

$$\begin{aligned}
H = & [A_1E + A_2A + A_2I + C_1u_1^2 + C_2u_2^2 + C_2u_3^2 + C_4u_4^2] + \\
& + \lambda_1 \left(\Lambda - \frac{\alpha(1-u_1)S(A+I)}{N} - (v(1+u_2) + \mu)S \right) \\
& + \lambda_2 \left(\frac{\alpha(1-u_1)S(A+I)}{N} - (\beta + \sigma + \mu)E \right) + \lambda_3 (\beta E - (\gamma + \delta + \mu)A) \\
& + \lambda_4 (\sigma E - (d + \mu + \eta(1+u_4))I) + \lambda_5 (\delta A - (\tau(1+u_3) + \mu)L) \\
& + \lambda_6 (v(1+u_2)S + \gamma A + \tau(1+u_3)L + \eta(1+u_4)I - \mu R),
\end{aligned} \tag{9}$$

According to model (9), we obtain a theorem for the existence of optimal control as follow.

Theorem 4. *There exists optimal control $u^* = (u_1^*, u_2^*, u_3^*, u_4^*) \in \Phi$ with initial condition $t_0 = 0$ and $J(u_1^*, u_2^*, u_3^*, u_4^*) = \min \{(u_1, u_2, u_3, u_4) : u_1, u_2, u_3, u_4 \in \Phi\}$.*

Proof:

System (5) are positive and set Φ is convex and close such that $A_1E + A_2A + A_2I + C_1u_1^2 + C_2u_2^2 + C_2u_3^2 + C_4u_4^2$ is convex function on Φ solution of system (5) are bounded, then Lipschitz of equality of the equation (6). There exists a constant $\omega > 1$ and positive number ξ_1, ξ_2 such that,

$$J((u_1, u_2, u_3, u_4) \geq \xi_1(|u_1|^2 + |u_2|^2 + |u_3|^2 + |u_4|^2)^{\frac{\omega}{2}} - \xi_2,$$

Then system (5) are bounded and there exists of optimal control of the system (5) is proven. \square

The Hamiltonian equation is derived for each subpopulation variable to minimize the equation (9) applied to Pontryagin's Maximum Principle, which is stated in the following theorem.

Theorem 5. *Let $S^*, E^*, A^*, I^*, L^*, R^*$ be the solutions of state variables associated with optimal control $u_1^*, u_2^*, u_3^*, u_4^*$, than it is obtained the co-state variables as follow.*

$$\begin{aligned}
\lambda_1' = & (\lambda_1 - \lambda_2) \left(\frac{\alpha(1-u_1)(A+I)}{N} \right) + (\lambda_1 - \lambda_6)(v(1+u_2) + \lambda_1\mu) \\
\lambda_2' = & -A_1 + (\lambda_2 - \lambda_3)\beta + (\lambda_2 - \lambda_4)\sigma + \lambda_2\mu \\
\lambda_3' = & -A_2 + (\lambda_1 - \lambda_2) \left(\frac{\alpha(1-u_1)S}{N} \right) + (\lambda_3 - \lambda_5)\delta + (\lambda_3 - \lambda_6)\gamma + \lambda_3\mu
\end{aligned} \tag{10}$$

$$\lambda'_4 = -A_3 + (\lambda_1 - \lambda_2) \left(\frac{\alpha(1-u_1)S}{N} \right) + (\lambda_4 - \lambda_6)\eta(1 + u_4) + \lambda_4(d + \mu)$$

$$\lambda'_5 = (\lambda_5 - \lambda_6)\tau(1 + u_3) + \lambda_5\mu$$

$$\lambda'_6 = \lambda_6\mu$$

with transversality conditions $\lambda_i(t_f) = 0, i = 1,2,3,4,5,6$, and control function $u_1^*, u_2^*, u_3^*, u_4^*$ is given

$$u_1^*(t) = \begin{cases} 0, & \text{if } \frac{\alpha(\lambda_2 - \lambda_1)S^*(A^* + I^*)}{2C_1N} \leq 0 \\ \frac{\alpha(\lambda_2 - \lambda_1)S(A+I)}{2C_1N}, & \text{if } 0 < \frac{\alpha(\lambda_2 - \lambda_1)S^*(A^* + I^*)}{2C_1N} < 1, \\ 1, & \text{if } \frac{\alpha(\lambda_2 - \lambda_1)S^*(A^* + I^*)}{2C_1N} \geq 1 \end{cases}$$

$$u_2^*(t) = \begin{cases} 0, & \text{if } \frac{(\lambda_1 - \lambda_6)vS^*}{2C_2} \leq 0 \\ \frac{(\lambda_1 - \lambda_6)vS^*}{2C_2}, & \text{if } 0 < \frac{(\lambda_1 - \lambda_6)vS^*}{2C_2} < 1, \\ 1, & \text{if } \frac{(\lambda_1 - \lambda_6)vS^*}{2C_2} \geq 1 \end{cases}$$

$$u_3^*(t) = \begin{cases} 0, & \text{if } \frac{(\lambda_5 - \lambda_6)\tau L^*}{2C_3} \leq 0 \\ \frac{(\lambda_5 - \lambda_6)\tau L^*}{2C_3}, & \text{if } 0 < \frac{(\lambda_5 - \lambda_6)\tau L^*}{2C_3} < 1, \\ 1, & \text{if } \frac{(\lambda_5 - \lambda_6)\tau L^*}{2C_3} \geq 1 \end{cases}$$

$$u_4^*(t) = \begin{cases} 0, & \text{if } \frac{(\lambda_4 - \lambda_6)\eta I^*}{2C_4} \leq 0 \\ \frac{(\lambda_4 - \lambda_6)\eta I^*}{2C_4}, & \text{if } 0 < \frac{(\lambda_4 - \lambda_6)\eta I^*}{2C_4} < 1. \\ 1, & \text{if } \frac{(\lambda_4 - \lambda_6)\eta I^*}{2C_4} \geq 1 \end{cases}$$

So, can are written as:

$$u_1^*(t) = \min \left\{ 1, \max \left(0, \frac{\alpha(\lambda_2 - \lambda_1)S^*(A^* + I^*)}{2C_1N} \right) \right\}$$

$$u_2^*(t) = \min \left\{ 1, \max \left(0, \frac{(\lambda_1 - \lambda_6)vS^*}{2C_2} \right) \right\}$$

$$u_3^*(t) = \min \left\{ 1, \max \left(0, \frac{(\lambda_5 - \lambda_6)\tau L^*}{2C_3} \right) \right\}$$

$$u_4^*(t) = \min \left\{ 1, \max \left(0, \frac{(\lambda_4 - \lambda_6)\eta I^*}{2C_4} \right) \right\}.$$

Proof. by deriving the Hamiltonian equation (9) with respect to each population variables, we obtain

PREVENTION AND TREATMENT OF COVID-19 SPREAD IN INDONESIA

$$\begin{aligned}\lambda'_1 &= -\frac{\partial H}{\partial S} = (\lambda_1 - \lambda_2) \left(\frac{\alpha(1-u_1)(A+I)}{N} \right) + (\lambda_1 - \lambda_6)(v(1+u_2) + \lambda_1\mu) \\ \lambda'_2 &= -\frac{\partial H}{\partial E} = -A_1 + (\lambda_2 - \lambda_3)\beta + (\lambda_2 - \lambda_4)\sigma + \lambda_2\mu \\ \lambda'_3 &= -\frac{\partial H}{\partial A} = -A_2 + (\lambda_1 - \lambda_2) \left(\frac{\alpha(1-u_1)S}{N} \right) + (\lambda_3 - \lambda_5)\delta + (\lambda_3 - \lambda_6)\gamma + \lambda_3\mu \\ \lambda'_4 &= -\frac{\partial H}{\partial I} = -A_3 + (\lambda_1 - \lambda_2) \left(\frac{\alpha(1-u_1)S}{N} \right) + (\lambda_4 - \lambda_6)\eta(1+u_4) + \lambda_4(d+\mu) \\ \lambda'_5 &= -\frac{\partial H}{\partial L} = (\lambda_5 - \lambda_6)\tau(1+u_3) + \lambda_5\mu \\ \lambda'_6 &= -\frac{\partial H}{\partial R} = \lambda_6\mu\end{aligned}$$

To prove the optimal control, based on the Hamiltonian equation (9), the change in each control

function remains constant, namely: $\frac{\partial H}{\partial u_1} = \frac{\partial H}{\partial u_2} = \frac{\partial H}{\partial u_3} = \frac{\partial H}{\partial u_4} = 0$. It is obtained

$$u_1^* = \frac{\alpha(\lambda_2 - \lambda_1)S^*(A^* + I^*)}{2C_1N}, \quad u_2^* = \frac{(\lambda_1 - \lambda_6)vS^*}{2C_2}, \quad u_3^* = \frac{(\lambda_5 - \lambda_6)\tau L^*}{2C_3}, \quad u_4^* = \frac{(\lambda_4 - \lambda_6)\eta I^*}{2C_4}$$

The upper bound is 1 lower bound is 0, for the controls u_1, u_2, u_3, u_4 and $u_i^* = u_i$, if $0 < u_i < 1$, $i = 1, 2, 3, 4$, we deduce the characterization.

$$\begin{aligned}u_1^*(t) &= \min \left\{ 1, \max \left(0, \frac{\alpha(\lambda_2 - \lambda_1)S^*(A^* + I^*)}{2C_1N} \right) \right\}, \quad u_2^*(t) = \min \left\{ 1, \max \left(0, \frac{(\lambda_1 - \lambda_6)vS^*}{2C_2} \right) \right\}, \\ u_3^*(t) &= \min \left\{ 1, \max \left(0, \frac{(\lambda_5 - \lambda_6)\tau L^*}{2C_3} \right) \right\}, \quad u_4^*(t) = \min \left\{ 1, \max \left(0, \frac{(\lambda_4 - \lambda_6)\eta I^*}{2C_4} \right) \right\}.\end{aligned}$$

The proof is complete. □

The basic reproduction number with control u_1, u_2, u_4 obtained as follows

$$R_{0\beta u_1, u_2} = \frac{\mu\alpha(1-u_1)\beta}{(v(1+u_2)+\mu)(\beta+\sigma+\mu)(\gamma+\delta+\mu)}, \quad R_{0\sigma u_1, u_2, u_4} = \frac{\mu\alpha(1-u_1)\sigma}{(v(1+u_2)+\mu)(\beta+\sigma+\mu)(d+\delta+\eta(1+u_4))}$$

It is clear that the controls reduce the magnitude of initial basic reproduction ratios.

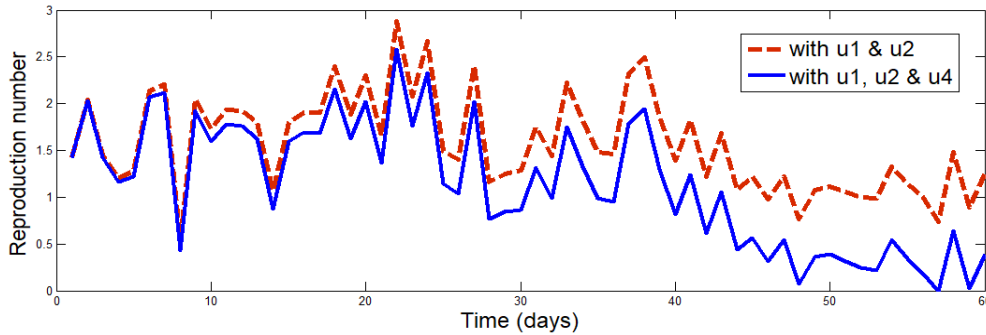


Figure 7. Reproduction number on the spread of COVID-19 in Indonesia on June 1- July 30, 2020

4. NUMERICAL SIMULATION OF OPTIMAL CONTROL

Numerical estimates used data from June 1 - July 31, 2020 in Indonesia. We use initial condition $(S(0), E(0), A(0), L(0), I(0), R(0)) = (26780411, 148401, 23601, 19759, 3842, 286)$, and total population $N(0)$ as 268,000,000. We use parameters' values as in Table 1.

In order to minimize the number of individuals who were confirmed positive, preventive controls (u_1, u_2) and treatment controls (u_3, u_4) were assigned, weighted administration costs for individuals subpopulation exposed, unreported infected and reported infected, respectively, namely: $A_1 = 100, A_2 = 10, A_3 = 200$. Campaign control administration costs (u_1) , vaccinated individual controls, self- isolated recovery controls (u_3) , infected and reported treatment controls (u_4) respectively in order: $C_1 = 50, C_2 = 100, C_3 = 150, C_4 = 200$. The solution to the optimal countermeasure control system (3.1), using the Runge-Kutha method of order 4 as in [20].

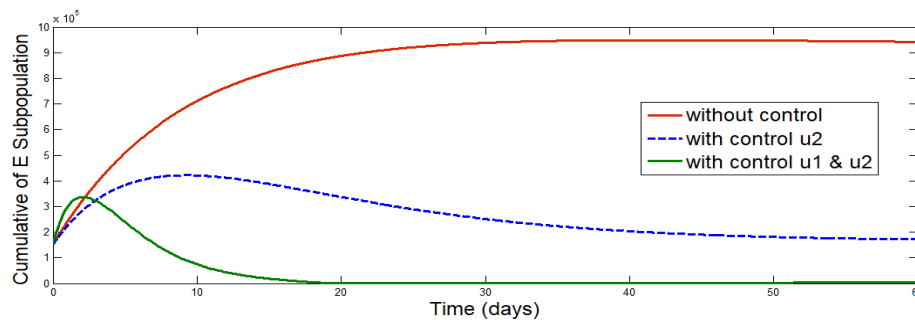


Figure 8. Dynamic of subpopulation E from 1 June 2020 to 31 July 2020 with and without control

Based on Figure 8, control u_2 can reduce the number of subpopulations E starting at time $t = 7$ days until $t = 60$ days. The number of individual compartments exposed decreases the number of individual compartments starting on day 3 and after day 20 the number of individual compartments E equals zero.

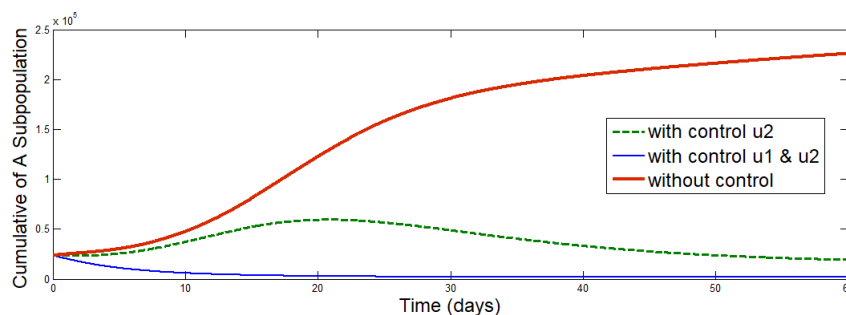


Figure 9. Dynamic of subpopulation A from 1 June 2020 to 31 July 2020 with and without control

In Figure 9, control u_2 can decrease the number of individual subpopulations A starting on day 30. Controls u_1 and u_2 together can reduce COVID-19 from day 1 to day 60. Based on Figure 10, controls u_1, u_2 and u_3 together reduce the number of infected I from $t = 10$ to $t = 60$ days, while the control u_1, u_2, u_3 and u_4 together can reduce infected individuals from day 1 to 60 days.

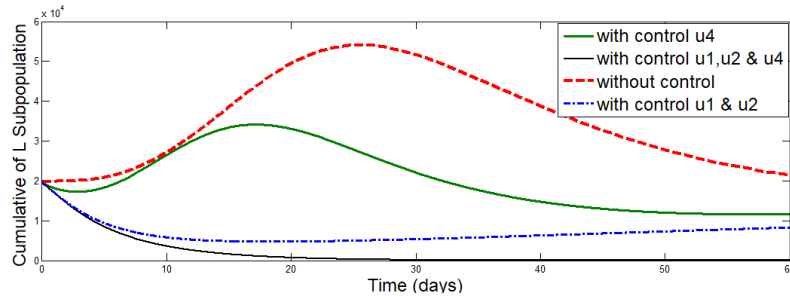


Figure 10: Dynamic of subpopulation I from 1 June 2020 to 31 July 2020 with and without control

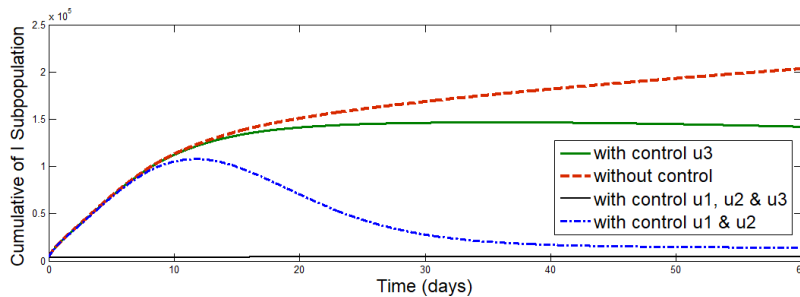


Figure 11. Dynamic of subpopulation L from 1 June 2020 to 31 July 2020 with and without control

Based on Figure 11, treatment control u_4 can reduce the number of COVID-19 individuals on day 15 to day 60. Control u_1 and u_2 can reduce the number of COVID-19 individuals slowly starting from the beginning until time $t = 60$ days. Control u_1, u_2, u_3 and u_4 together can reduce infected individuals from day 1 to time $t = 30$ days and the number of infected zero after time $t = 30$ to $t = 60$ days.

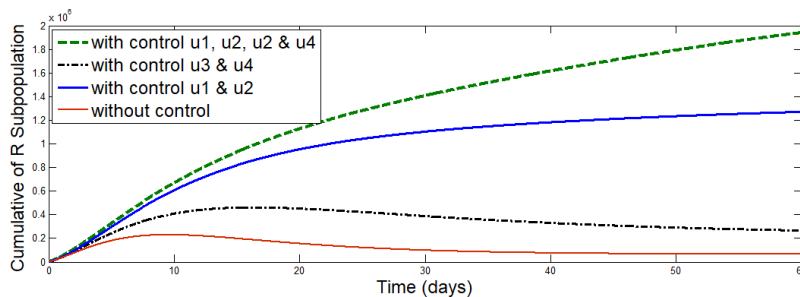


Figure 12. Dynamic of subpopulation R from 1 June 2020 to 31 July 2020 with and without control

Based on Figure 12, preventive controls u_1 and u_2 better increase the number of individuals who recover from COVID-19 compared to treatment controls u_3 and u_4 . The control u_1, u_2, u_3 and u_4 together were better at improving individuals who recovered from COVID-19 compared to the control u_1 and u_2 or control u_3 and u_4 .

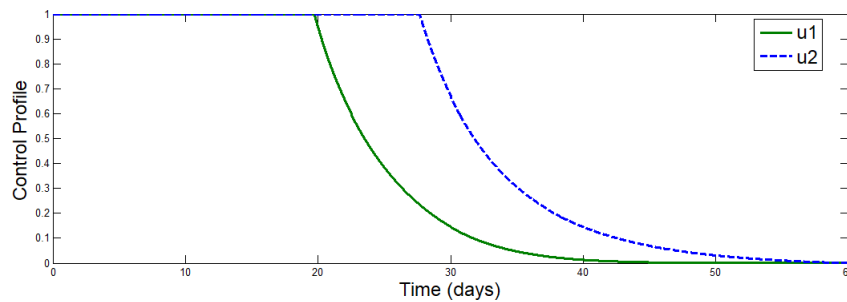


Figure 13. Profile of prevention controls u_1, u_2 .

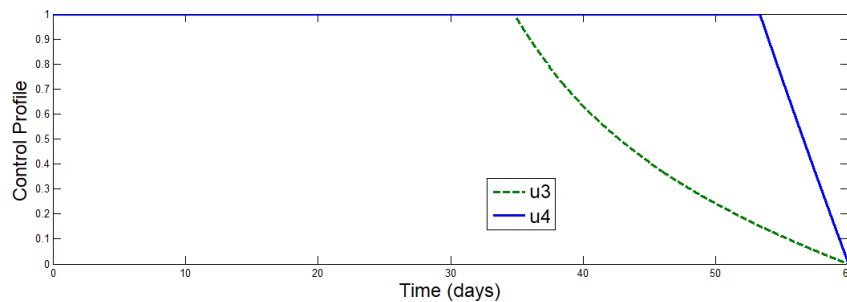


Figure 14. Profile of treatment controls u_3, u_4 .

Figure 13 is a preventative control. Optimal control u_1 reduces COVID-19 at baseline until time $t = 20$, after $t = 20$ decreases until $t = 60$ days, optimal control u_2 reduces COVID-19 from baseline to $t = 28$, after $t = 28$ decreased to $t = 60$ days.

Figure 14 is treatment control, optimal control u_3 reduces COVID-19 from baseline to $t = 35$ days, after $t = 35$ decreases to $t = 60$ days, optimal control u_4 decreased COVID-19 from the beginning to $t = 53$ days, after $t = 53$ decreased to $t = 60$ days.

5. CONCLUSION

Based on the analysis of the model obtained non-endemic and endemic equilibrium points. The basic reproduction ratio of the model is obtained using the next generation matrix. The non-endemic equilibrium point in the local asymptotically stable system of equations (1), and

the endemic equilibrium point in the local asymptotically stable system of equations (1) based on the Routh-Hurwitz criteria.

The optimal control characterization analysis obtained the conditions for the existence of optimal control, from the solution of state variables associated with optimal control obtained co-state variables. Based on the Hamiltonian equation, the optimal control for the prevention and treatment of COVID-19 and the existence of co-states for each subpopulation is obtained. Numerical simulation of the basic reproduction number parameter, the value of the reproduction ratio with control is smaller than without control, meaning that by using optimal prevention and treatment controls, the spread of COVID-19 can be reduced. Preventive control optimal (u_1 and u_2) were more efficient in reducing the number of individuals infected with COVID-19 compared to using treatment controls (u_3 and u_4). The control u_1 , u_2 , u_3 and u_4 together were better at improving individuals who recovered from COVID-19 compared to the control u_1 and u_2 or control u_3 and u_4 .

CONFLICT OF INTERESTS

The authors declare that there is no conflict of interests.

ACKNOWLEDGEMENT

The authors would like to thank Kemenristek Dikti providing Higher Education Grants of College Leading Basic Research for Fiscal Year 2022, through LPPM Universitas Cenderawasih who sponsored the research.

REFERENCES

- [1] N. Anggriani, M.Z. Ndi, R. Amelia, et al. A mathematical COVID-19 model considering asymptomatic and symptomatic classes with waning immunity, Alexandria Eng. J. 61 (2022), 113–124.
<https://doi.org/10.1016/j.aej.2021.04.104>.
- [2] T.M. Chen, J. Rui, Q.P. Wang, et al. A mathematical model for simulating the phase-based transmissibility of a novel coronavirus, Infect. Dis. Poverty. 9 (2020), 24. <https://doi.org/10.1186/s40249-020-00640-3>.

- [3] D. Dwomoh, S. Iddi, B. Adu, et al. Mathematical modeling of COVID-19 infection dynamics in Ghana: Impact evaluation of integrated government and individual level interventions, *Infect. Dis. Model.* 6 (2021), 381–397. <https://doi.org/10.1016/j.idm.2021.01.008>.
- [4] E.A. Iboi, O. Sharomi, C.N. Ngonghala, et al. Mathematical modeling and analysis of COVID-19 pandemic in Nigeria, *Math. Biosc. Eng.* 17 (2020), 7193–7221. <https://doi.org/10.3934/mbe.2020369>.
- [5] K.M. O'Reilly, F. Sandman, D. Allen, et al. Predicted norovirus resurgence in 2021–2022 due to the relaxation of nonpharmaceutical interventions associated with COVID-19 restrictions in England: a mathematical modeling study, *BMC Med.* 19 (2021), 299. <https://doi.org/10.1186/s12916-021-02153-8>.
- [6] I.H.K. Premarathna, H.M. Srivastava, Z.A.M.S. Juman, et al. Mathematical modeling approach to predict COVID-19 infected people in Sri Lanka, *AIMS Math.* 7 (2022), 4672–4699. <https://doi.org/10.3934/math.2022260>.
- [7] A. Zeb, E. Alzahrani, V.S. Erturk, et al. Mathematical model for coronavirus disease 2019 (COVID-19) containing isolation class, *BioMed Research International.* 2020 (2020) 3452402. <https://doi.org/10.1155/2020/3452402>.
- [8] X. Yu, L. Lu, J. Guo, et al. VSHR: A mathematical model for the prediction of second-wave COVID-19 epidemics in Malaysia, *Comput. Math. Method Med.* 2022 (2022), 4168619. <https://doi.org/10.1155/2022/4168619>.
- [9] L. Basnarkov, SEAIR Epidemic spreading model of COVID-19, *Chaos Solitons Fractals.* 142 (2021), 110394. <https://doi.org/10.1016/j.chaos.2020.110394>.
- [10] J. Nainggolan, Moch.F. Ansori, Stability and Sensitivity Analysis of the COVID-19 Spread with Comorbid Diseases, *Symmetry.* 14 (2022), 2269. <https://doi.org/10.3390/sym14112269>.
- [11] S.S. Musa, S. Qureshi, S. Zhao, et al. Mathematical modeling of COVID-19 epidemic with effect of awareness programs, *Infect. Dis. Model.* 6 (2021), 448–460. <https://doi.org/10.1016/j.idm.2021.01.012>.
- [12] B. Ivorra, M.R. Ferrández, M. Vela-Pérez, et al. Mathematical modeling of the spread of the coronavirus disease 2019 (COVID-19) taking into account the undetected infections. The case of China, *Commun. Nonlinear Sci. Numer. Simul.* 88 (2020), 105303. <https://doi.org/10.1016/j.cnsns.2020.105303>.

PREVENTION AND TREATMENT OF COVID-19 SPREAD IN INDONESIA

- [13] S.S. Nadim, J. Chattopadhyay, Occurrence of backward bifurcation and prediction of disease transmission with imperfect lockdown: A case study on COVID-19, *Chaos Solitons Fractals*. 140 (2020), 110163.
<https://doi.org/10.1016/j.chaos.2020.110163>.
- [14] S. Annas, M.I. Pratama, M. Rifandi, et al. Stability analysis and numerical simulation of SEIR model for pandemic COVID-19 spread in Indonesia, *Chaos Solitons Fractals*. 139 (2020), 110072.
<https://doi.org/10.1016/j.chaos.2020.110072>.
- [15] O.J. Peter, S. Qureshi, A. Yusuf, et al. A new mathematical model of COVID-19 using real data from Pakistan, *Results Phys*. 24 (2021), 104098. <https://doi.org/10.1016/j.rinp.2021.104098>.
- [16] A. Ahmed, B. Salam, M. Mohammad, et al. Analysis coronavirus disease (COVID-19) model using numerical approaches and logistic model, *AIMS Bioeng*. 7 (2020), 130–146. <https://doi.org/10.3934/bioeng.2020013>.
- [17] B.N. Kim, E. Kim, S. Lee, et al. Mathematical model of COVID-19 transmission dynamics in South Korea: The impacts of travel restrictions, social distancing, and early detection, *Processes*. 8 (2020), 1304.
<https://doi.org/10.3390/pr8101304>.
- [18] Y. Liu, A.A. Gayle, A. Wilder-Smith, J. Rocklöv, The reproductive number of COVID-19 is higher compared to SARS coronavirus, *J. Travel Med*. 27 (2020), taaa021. <https://doi.org/10.1093/jtm/taaa021>.
- [19] N.R. Sasmita, M. Ikhwan, S. Suyanto, et al. Optimal control on a mathematical model to pattern the progression of coronavirus disease 2019 (COVID-19) in Indonesia, *Glob. Health Res. Policy*. 5 (2020), 38.
<https://doi.org/10.1186/s41256-020-00163-2>.
- [20] S. Nana-Kyere, F.A. Boateng, P. Jonathan, et al. Global analysis and optimal control model of COVID-19, *Comput. Math. Methods Med*. 2022 (2022), 9491847. <https://doi.org/10.1155/2022/9491847>.
- [21] S.R. Bandekar, M. Ghosh, Mathematical modeling of COVID-19 in India and its states with optimal control, *Model. Earth Syst. Environ*. 8 (2021), 2019–2034. <https://doi.org/10.1007/s40808-021-01202-8>.
- [22] A.I. Abioye, O.J. Peter, H.A. Ogunseye, F.A. Oguntolu, K. Oshinubi, A.A. Ibrahim, I. Khan, Mathematical model of COVID-19 in Nigeria with optimal control, *Results Phys*. 28 (2021) 104598.
<https://doi.org/10.1016/j.rinp.2021.104598>.

- [23] F. Inayaturohmat, N. Anggriani, A.K. Supriatna, Optimal control and sensitivity analysis of COVID-19 transmission model with the presence of waning immunity in West Java, Indonesia, *Commun. Math. Biol. Neurosci.* 2022 (2022), 19. <https://doi.org/10.28919/cmbn/7124>.
- [24] P. van den Driessche, J. Watmough, Reproduction numbers and sub-threshold endemic equilibria for compartmental models of disease transmission, *Math. Biosci.* 180 (2002), 29–48. [https://doi.org/10.1016/s0025-5564\(02\)00108-6](https://doi.org/10.1016/s0025-5564(02)00108-6).
- [25] J. Nainggolan, Fatmawati, Optimal prevention strategy of the type SIR COVID-19 spread model in Indonesia, *Commun. Math. Biol. Neurosci.* 2021 (2021), 46. <https://doi.org/10.28919/cmbn/5571>.
- [26] C. Castillo-Chavez, Z. Feng, W. Huang, On the computation of R_0 and its role on global stability, in: C. Castillo-Chavez, S. Blower, P. van den Driessche, D. Kirschner, A.-A. Yakubu (Eds.), *Mathematical Approaches for Emerging and Reemerging Infectious Diseases: An Introduction*, Springer New York, 2002: pp. 229–250. https://doi.org/10.1007/978-1-4757-3667-0_13.